

Dispersion Method for Safety Research on Manufactured Nanomaterials

Wenting WU^{1,2}, Gaku ICHIHARA^{1*}, Yuka SUZUKI², Kiyora IZUOKA², Saeko OIKAWA-TADA², Jie CHANG^{1,2}, Kiyoshi SAKAI³, Kunichi MIYAZAWA⁴, Dale PORTER⁵, Vincent CASTRANOVA⁵, Masami KAWAGUCHI⁶ and Sahoko ICHIHARA²

¹Department of Occupational and Environmental Health, Nagoya University Graduate School of Medicine, Japan

²Graduate School of Regional Innovation Studies, Mie University, Japan

³Nagoya City Public Health Research Institute, Japan

⁴National Institute for Materials Science, Japan

⁵National Institute for Occupational Safety and Health, USA

⁶Division of Chemistry for Materials, Graduate School of Engineering, Mie University, Japan

Received December 24, 2012 and accepted November 22, 2013

Published online in J-STAGE December 4, 2013

Abstract: Nanomaterials tend to agglomerate in aqueous media, resulting in inaccurate safety assessment of the biological response to these substances. The present study searched for suitable dispersion methods for the preparation of nanomaterial suspensions. Titanium dioxide (TiO₂) and zinc oxide (ZnO) nanoparticles were dispersed in a biocompatible dispersion medium by direct probe-type sonicator and indirect cup-type sonicator. Size characterization was completed using dynamic light scattering and transmission electron microscopy. A series of dispersion time and output power, as well as two different particle concentrations were tested. Microscopic contamination of metal titanium that broke away from the tip of the probe into the suspension was found. Size of agglomerated nanoparticles decreased with increase in sonication time or output power. Particle concentration did not show obvious effect on size distribution of TiO₂ nanoparticles, while significant reduction of secondary diameter of ZnO was observed at higher concentration. A practicable protocol was then adopted and sizes of well-dispersed nanoparticles increased by less than 10% at 7 d after sonication. Multi-walled carbon nanotubes were also well dispersed by the same protocol. The cup-type sonicator might be a useful alternative to the traditional bath-type sonicator or probe-type sonicator based on its effective energy delivery and assurance of suspension purity.

Key words: Nanomaterials, Nanoparticles, Carbon nanotubes, Safety research, Suspension, Dispersion, Sonication

Introduction

According to the European Commission, nanomaterial is defined as a material containing particles with

one or more external dimensions in the size range of 1–100 nm¹⁾. The remarkable revolution in nanotechnology shows promising potential applications of manufactured nanomaterials in a variety of areas including engineering, medicine, consumer, and information technology^{2, 3)}. On the other hand, safety evaluation of manufactured nanomaterials is urgently required because of the considerable probability of occupational and environmental exposure

*To whom correspondence should be addressed.

E-mail: gak@med.nagoya-u.ac.jp

©2014 National Institute of Occupational Safety and Health

throughout the product chain during manufacture, application and waste management^{2, 4}). Furthermore, there is increasing concern that the novel physico-chemical properties of nanomaterials that are different from those of bulk materials might have unpredictable health effects^{5, 6}).

Both *in vivo* and *in vitro* studies demonstrated that the higher toxicity of nanomaterials was correlated with the relatively larger surface area derived from their smaller sizes⁷⁻¹¹). However, nanomaterials tend to agglomerate into micrometer-sized structures in aqueous media, subsequently exerting different biological effects compared to well-dispersed ones, probably due to the ineffective surface area delivered by the poor dispersed suspension¹²⁻¹⁵). Therefore, the selection of suitable dispersion methods is important for accurate evaluation of toxicological responses to nanomaterials.

In safety research on nanomaterials, sonication is the most widely used procedure to accomplish a suspension¹⁶⁻²⁰). Cavitation from alternating high and low pressure cycles provides energy that facilitates the disruption of agglomerates. Agglomerates of particles bound together by relatively weak forces, such as Van der Waals forces, can be fragmented by sonication, while aggregates created by stronger chemical bonds are difficult to be broken down²¹). Instead of electrostatic stabilization, steric stabilization by adding stabilizers into the suspension is often used to maintain homogeneous dispersion induced by sonication. Pulmonary surfactant, albumin, cell culture medium, and serum have been reported to prevent nanomaterials from approaching each other by formation of a protein corona, contributing to the suppression of gross cluster formation and the improvement of suspension stability^{13, 22, 23}).

Recent studies have shown that exposure to various kinds of nanomaterials, such as metal oxide nanoparticles, carbon nanoparticles and nanotubes is injurious to biological systems²⁴⁻²⁹). In addition to the gastrointestinal track and skin, the respiratory system is recognized as one of the most important portals of entry and a target tissue, and a number of *in vivo* research studies have focused on the respiratory system to investigate the harmful effects of airborne nanomaterials^{14, 30, 31}). For the evaluation of respiratory toxicity, intratracheal instillation/spray and pharyngeal aspiration are useful and cost-effective exposure techniques routinely used in investigative exposure of animals to particles³²⁻³⁷). The dispersion medium (DM), an artificial physiological buffer comprised of protein and surfactant components naturally found in lung alveolar fluids, which are known to be effective in both reduction

of agglomeration and stabilization of suspensions, was recommended in the preparation of nanomaterials suspension in pulmonary exposure studies using intratracheal instillation/spray or pharyngeal aspiration³⁸).

The aim of the present study was to investigate the factors that influence the dispersion status and establish a suitable and reproducible protocol for the preparation of nanomaterial suspensions specific for pulmonary exposure studies. Two kinds of different nanospheres and one kind of carbon nanotube were dispersed in DM by a direct probe-type sonicator or indirect cup-type sonicator. A series of sonication times and output powers, as well as two different dispersion concentrations of particle suspension were tested. Size characterization was completed by dynamic light scattering (DLS) and further examined morphologically with a transmission electron microscope (TEM). Dispersion stability over time was also assessed.

Subjects and Methods

Nanomaterials

Titanium dioxide (TiO₂) nanoparticles (AEROXIDE TiO₂ P25; Degussa AG, Dusseldorf, Germany) with a primary diameter of 21 nm, zinc oxide (ZnO) nanoparticles (MKN-ZnO-020; mkNano, Mississauga, ONT, Canada) with a primary diameter of 20 nm, and multi-walled carbon nanotubes (MITSUI MWCNT-7; Mitsui, Tokyo, Japan) with a diameter of 100 nm and length of 27% >5 μm were used in the present study. The selection of 20 nm for ZnO nanoparticles was based on the similarity of the diameter to that of P25 TiO₂ nanoparticles. The nanomaterials were stored in 50-ml polypropylene conical tubes until use.

Dispersion medium (DM)

Porter *et al.*³⁸) demonstrated that DM neither caused pulmonary inflammation or cytotoxicity, nor altered the toxicity of tested silica particles, suggesting that DM is an effective, biocompatible and economical vehicle for nanotoxicological evaluation. DM was prepared as described previously. Briefly, Ca²⁺ and Mg²⁺-free phosphate buffered saline (PBS) was supplemented with 5.5 mM D-glucose, 0.6 mg/ml bovine serum albumin (BSA), and 0.01 mg/ml 1, 2-dipalmitoyl-sn-glycero-3-phosphocholine (DPPC), and sonicated for 10 min with continuous 70 W output power by bath-type sonicator after mixing. DM was prepared within 2 days before dispersion and stored in a refrigerator at 4°C.

Suspension

Dispersion of nanomaterial suspensions were performed in a 50-ml polypropylene conical tube. In terms of probe-type sonicator, we used the ultrasonic system (Sonifier 450 Advances; Branson, Danbury, CT) with a horn having a tip diameter of 1/2" (13 mm). Particles were dispersed in 20 ml of DM and the tube was immersed in an ice-salt bath during sonication. For the cup-type sonicator (cup horn; Branson), a circulatory cooling system was used to avoid over heating of the suspension. When the tube is immersed into the circulatory cooling water in the sonicator, the maximum volume of suspension in the tube to be covered by the cooling water is 8 ml, and therefore the volume of DM was adjusted to 8 ml. Output power was determined by the sonicator dial according to the manual provided by the manufacturer.

Size characterization

Soon after sonication, dispersed suspensions of 25 $\mu\text{g/ml}$ TiO₂ (absorbance: 0.010; refractive index: 2.520) and 500 $\mu\text{g/ml}$ ZnO (absorbance: 0.010; refractive index: 2.020) were prepared in DM (viscosity: 1.0; refractive index: 1.33), and then vortexed and filtered through a 0.6 μm isopore membrane filter (Merk Millipore, Billerica, MA) into a disposable standard cuvette. Each sample was measured by dynamic light scattering (DLS) (Zetasizer Nano-S; Malvern Instruments, Worcestershire, UK) at 25°C four times after 1 h on standing. Dispersion status was described as the peak value of the principal peak of the intensity-weighted hydrodynamic diameter distribution (peak 1), in conjunction with polydispersity index (PDI), which reflected the broadness of the size distribution (scale range from 0 to 1, with 0 being monodispersion and 1 being polydispersion)²².

To check the stability of the suspension, size characterization was conducted soon after, and at 1, 3, and 7 days post-sonication (ZnO was not measured at 3 days post-sonication because of inadequacy of samples). The prepared dispersions were stored in a refrigerator at 4°C until measured, and after vortexing for several seconds they were subsequently analyzed by DLS as mentioned previously.

Morphological characterization

A drop (approximately 0.1 ml) of each sample was deposited onto an elastic carbon-coated copper grid or high-resolution carbon-coated copper grid to observe the dispersed TiO₂ or MWCNT, respectively, and allowed to air dry. A transmission electron microscope (TEM, JEM-1011; JEOL, Tokyo) was used to visualize the dispersed nanomaterials. MWCNT suspensions were also viewed

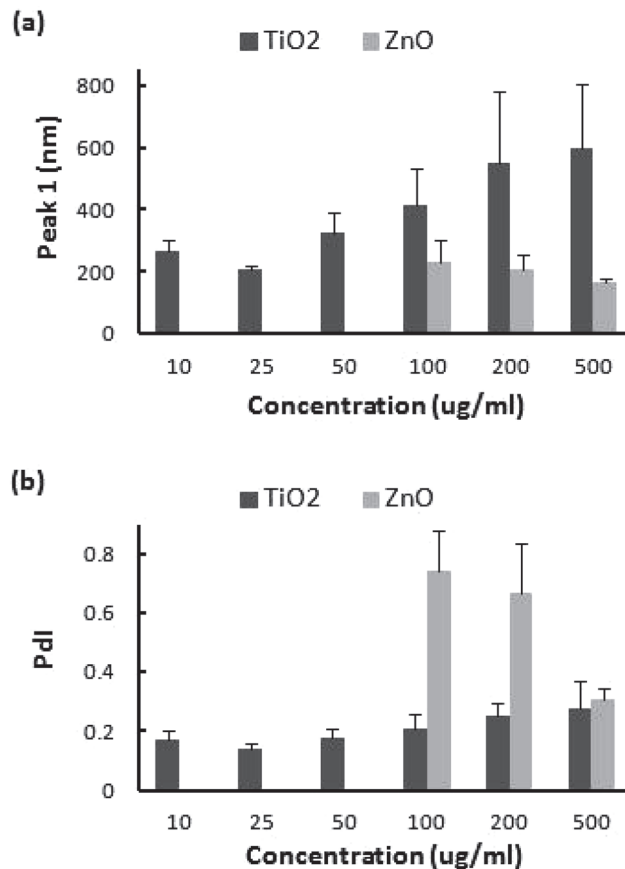


Fig. 1. Size characterization of TiO₂ and ZnO nanoparticle suspensions at concentration of 0.5 mg/ml dispersed by a probe-type sonicator at 20 W, 80% pulse mode, for 30 min, being measured by DLS at concentrations of 10, 25, 50, 100, 200, and 500 $\mu\text{g/ml}$: (a) peak 1 and (b) PDI. Data are mean \pm SD.

using an Olympus BXJ1 optical microscope (OLYMPUS, Tokyo) equipped with a digital camera DP70, to capture images with the DP controller software (OLYMPUS).

Results

Direct probe-type sonicator

Particle concentration for DLS measurement

Suspensions of TiO₂ and ZnO nanoparticles at a concentration of 0.5 mg/ml were dispersed by probe-type sonicator at 20 W, 80% pulse mode, for 5, 10, 20, or 30 min. The sample dispersed for 30 min was diluted with DM into concentrations of 10, 25, 50, 100, 200 and 500 $\mu\text{g/ml}$ (ZnO nanoparticles were tested at concentrations of 100, 200 and 500 $\mu\text{g/ml}$), and peak1 and PDI values were determined for each concentration sample (Fig. 1).

TiO₂ nanoparticles showed the smallest peak1 and PDI at the concentration of 25 $\mu\text{g/ml}$. At particle concentrations

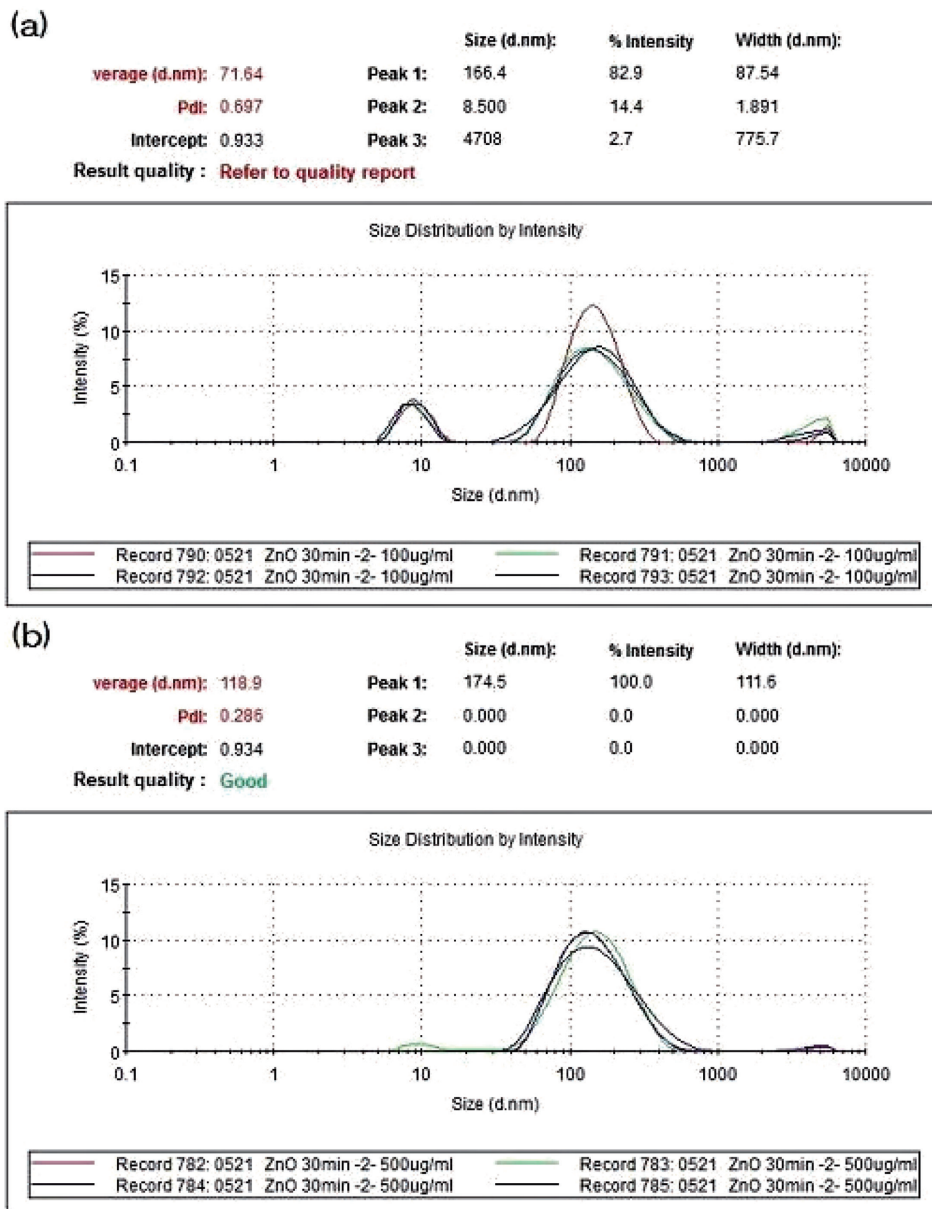


Fig. 2. Report of size distribution of ZnO nanoparticles suspensions dispersed by a probe-type sonicator at 20 W, 80% pulse mode, for 30 min, at measure concentrations of: (a) 100 and (b) 500 $\mu\text{g/ml}$.

ranging from 25 to 500 $\mu\text{g/ml}$, the secondary hydrodynamic diameter increased with elevated concentration. The coefficient of variation of peak1 was 12.63, 5.18, 19.26, 25.50, 42.24 and 34.82% at concentrations of 10, 25, 50, 100, 200 and 500 $\mu\text{g/ml}$, respectively, indicating the least deviation of size distribution at the concentration of 25 $\mu\text{g/ml}$.

On the contrary, peak 1 and its standard deviation of ZnO nanoparticles slightly decreased with elevated particle concentration, and Pdi of ZnO also decreased depending on the particle concentration to a greater extent than the

peak 1 of ZnO. The size distribution provided by DLS (Fig. 2) showed unimodal distribution at the concentration of 500 $\mu\text{g/ml}$, while there was a small sub-peak around 8 nm at 100 $\mu\text{g/ml}$. The size distribution of DM was measured to confirm that the peak around 8 nm was derived from DM (data not shown).

Dispersion time

Suspensions of TiO_2 and ZnO nanoparticles at concentration of 0.5 mg/ml were dispersed by probe-type sonicator at 20 W, 80% pulse mode, for 5, 10, 20, or

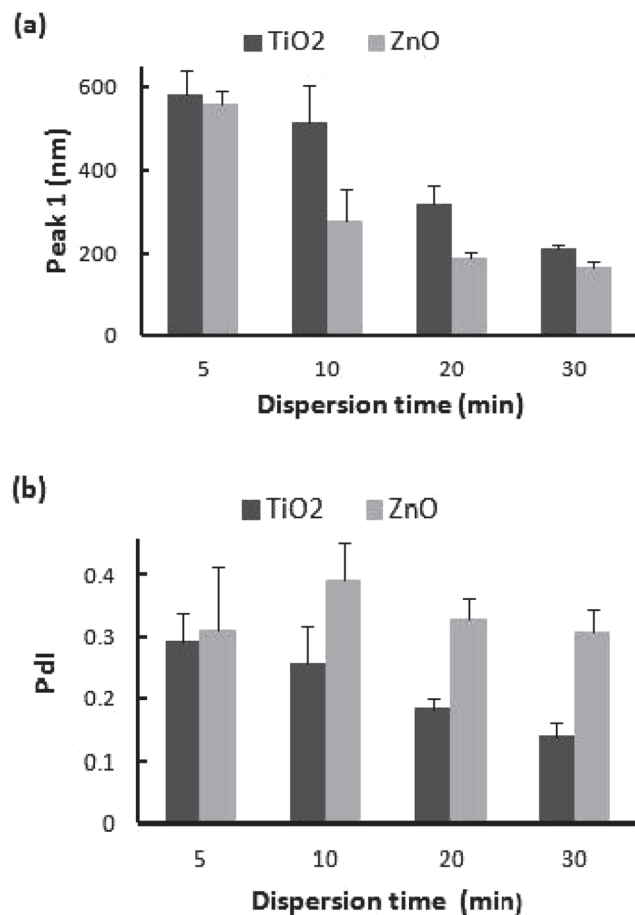


Fig. 3. Size characterization of TiO₂ and ZnO nanoparticle suspensions at concentration of 0.5 mg/ml dispersed by a probe-type sonicator at 20 W, 80% pulse mode for 5, 10, 20, or 30 min: (a) peak 1 and (b) PDI. Data are mean \pm SD.

30 min. With increased dispersion time, DLS measurement showed a decrease in hydrodynamic diameter of both TiO₂ and ZnO nanoparticles, as well as tendency toward monodispersion of TiO₂ nanoparticles and decreased standard deviation of PDI of ZnO nanoparticles (Fig. 3). TEM showed the presence of smaller TiO₂ nanoparticle agglomerates in 30-min sonicated samples (Fig. 4 (b)) compared with the large agglomerates found after sonication for 10 min (Fig. 4 (a)). These results suggest that longer dispersion time allowed the delivery of more energy to break the bonds within the agglomerates. After filtration, poor dispersion suspension (5 or 10 min) appeared more limpid, probably due to the retention of larger number of micro-sized agglomerates on the filter membrane. In comparison, samples sonicated for 30 min appeared turbid and this indicated that the majority of small agglomerates distributed well in the dispersed suspension (Fig. 5).

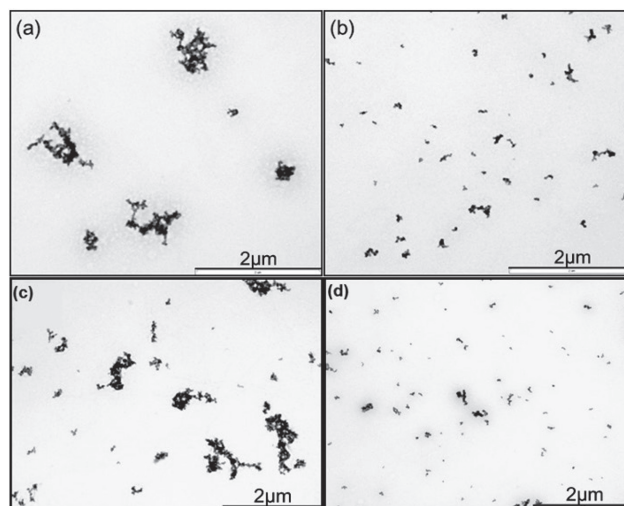


Fig. 4. TEM micrographs of TiO₂ nanoparticle suspensions at concentration of 0.5 mg/ml dispersed by (A) a probe-type sonicator at 20 W, 80% pulse mode, for (a) 10 min and (b) 30 min; (B) a cup-type sonicator at (c) 50 W and (d) 100W, 80% pulse mode, for 10 min.

Contamination from the probe

Black sediment was found at the bottom of the samples sonicated for 30 min after 2 h on standing (Fig. 6 (a)). Inspection of the surface of the probe tip showed abrasion, which was probably due to the intense cavitation (Fig. 6 (b)). These microscopic tip residues of titanium were presumed to be broken away from the tip into the suspension.

Indirect cup-type sonicator

Temperature of cooling water

Suspensions of TiO₂ nanoparticles at concentration of 0.5 mg/ml were dispersed by cup-type sonicator at 220 W (max), 80% pulse mode. For the purpose of suppression of sample heating, a circulatory cooling system consisting of a congealer that circulated 30% ethanol with a pump at the flow rate of 400 ml/min was utilized. At the beginning, we attempted to lower the temperature of cooling water to -10°C so that sonication was able to be carried out with long dispersion time. When sonicated for 40 min, agglomerated TiO₂ nanoparticles were dispersed into 371.8 ± 12.5 nm with PDI of 0.24 ± 0.01 when the circulation temperature was set at -10°C , and the sample temperature was measured lower than the room temperature (25°C) after dispersion. In contrast, when the circulation temperature was set at 5°C , particles were dispersed into 173.9 ± 12.8 nm with PDI of 0.15 ± 0.01 after 10-minute sonication, and the sample was heated to 37.6°C . In spite of the shorter dispersion time, sonication at a relatively higher temperature (5°C) produced better monodispersion of

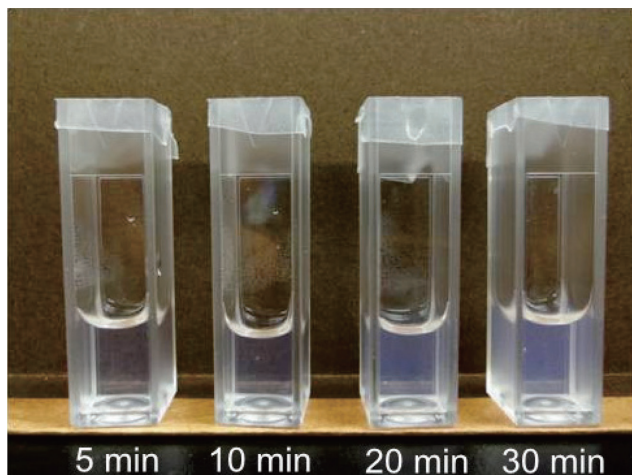


Fig. 5. Change in the turbidity of filtered TiO₂ nanoparticle suspensions dispersed by a probe-type sonicator at 20 W, 80% pulse mode, for 5, 10, 20, or 30 min at concentration of 0.5 mg/ml.

small agglomerates, suggesting that the cup-type sonication system should be cooled to moderate temperatures only. Since the sample was extremely caustic at dispersion time longer than 10 min, we chose a dispersion time of 10 min for the suspension using the cup-type sonicator.

Output power of sonicator

Suspensions of TiO₂ and ZnO nanoparticles at concentration of 0.5 mg/ml were dispersed by the cup-type sonicator at 10, 20, 50, 100, or 220 W, 80% pulse mode, for 10 min (Fig. 7). The size of the sonicated TiO₂ nanoparticles appeared to decrease with increased output power, although the maximum reduction reached a plateau level at output power of 100 W, and a similar trend was noted for PDI. More energy delivered with higher output power facilitated disruption of agglomeration and output power of 100W was deemed likely to be adequate for dispersion of TiO₂ nanoparticles. TEM micrographs of the samples sonicated at 50 or 100 W confirmed the results of DLS (Fig. 4).

Surprisingly, output power ranging from 10 to 220 W had little effect on sizes of agglomerated ZnO nanoparticles, while PDI showed an output power-dependent decrease from 10 to 50 W. The energy delivered with output power of 10 W might be enough for agglomerate breakage, but output power less than 50 W was insufficient to accomplish monodispersion.

Determination of dispersion time for nanoparticles

We also compared the size distribution between samples sonicated at 220 W, 80% pulse mode for 10 min and that

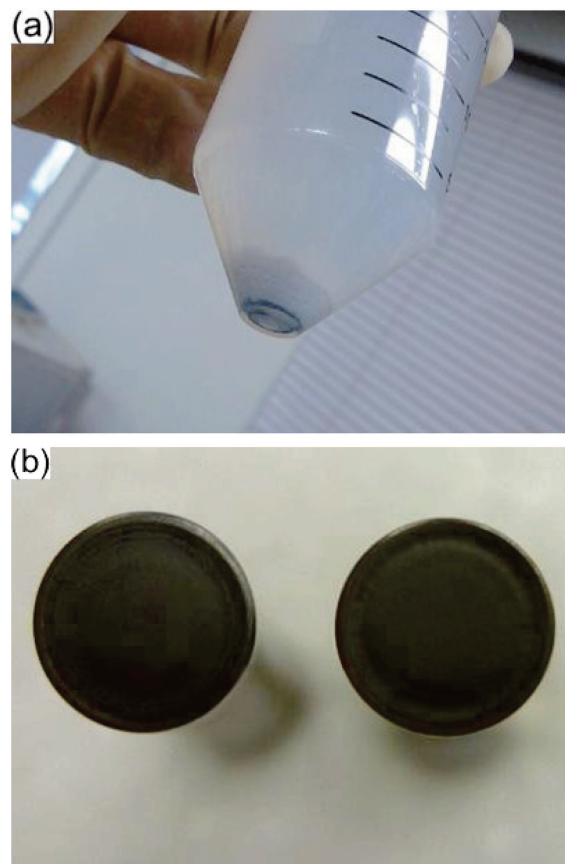


Fig. 6. (a) Black sediment at the bottom of a sample sonicated by a probe-type sonicator at 20 W, 80% pulse mode, for 30 min after 2 hours on standing and (b) the tip surface of unused probe (left) and abraded probe (right).

of samples sonicated several times each for 10 min, with sample cooling in between the sonications. The size of agglomerated TiO₂ nanoparticles sonicated four times each for 10 min was 182.2 ± 0.6 nm, which was similar to 173.9 ± 12.8 nm obtained after a single sonication. Regarding ZnO nanoparticles, one single sonication for 10 min dispersed the agglomerates into 180.2 ± 5.0 nm and three-time sonication also yielded a similar result of 177.5 ± 1.5 nm. This phenomenon was deduced to be the result of the balance between deagglomeration and reagglomeration taking place during the process of delivered energy elevation²¹). It seemed that sonication at 220 W, 80% pulse mode, for 10 min was favorable for the dispersion of these two nanoparticles.

Applicability

Particle concentration for dispersion

Suspensions of TiO₂ and ZnO nanoparticles at concentrations of 0.5 or 2.5 mg/ml were dispersed by the cup-

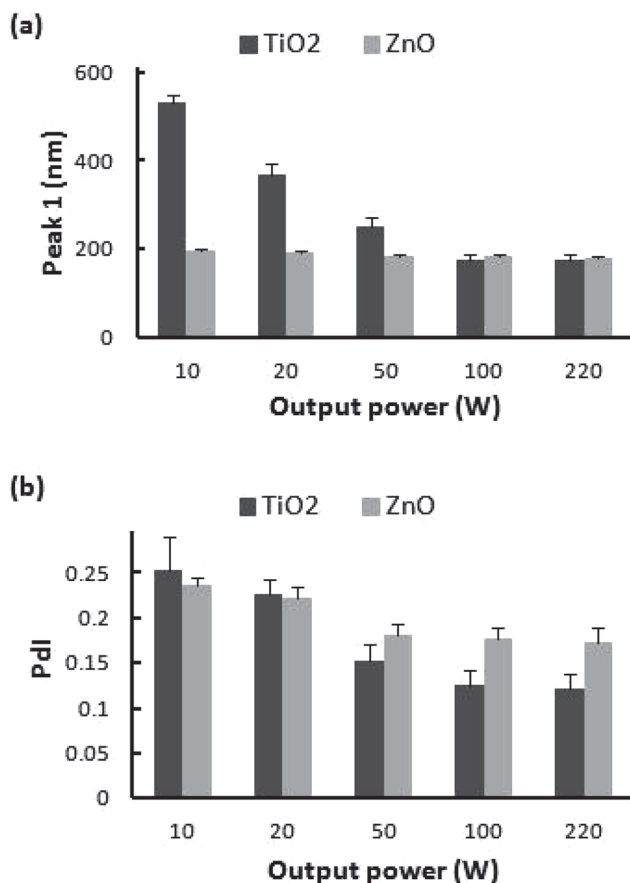


Fig. 7. Size characterization of TiO₂ and ZnO nanoparticle suspensions at concentration of 0.5 mg/ml dispersed by a cup-type sonicator at 10, 20, 50, 100, or 220 W, 80% pulse mode, for 10 min: (a) peak 1 and (b) Pdl. Data are mean \pm SD.

Table 1. Effect of particle concentration for dispersion

Nanoparticle	Concentration (mg/ml)			
	0.5		2.5	
	Peak 1 (nm)	Pdl	Peak 1 (nm)	Pdl
TiO ₂	173.9 \pm 12.8	0.12 \pm 0.02	180.8 \pm 31.4	0.13 \pm 0.02
ZnO	180.2 \pm 5.0	0.18 \pm 0.01	169.8 \pm 3.1*	0.17 \pm 0.02

Data are mean \pm SD; * $p < 0.05$.

Table 2. Stability of nanoparticle suspensions

Particles	Output power	Peak 1 (nm)			
		0 d	1 d	3 d	7 d
TiO ₂	100 W	174.0 \pm 12.3	182.1 \pm 14.6	187.5 \pm 19.2	190.0 \pm 20.6
	220 W	173.9 \pm 12.8	176.5 \pm 13.6	184.1 \pm 11.8	181.7 \pm 16.2
ZnO	100 W	177.2 \pm 4.7	180.6 \pm 4.7	/	183.3 \pm 4.9
	220 W	180.2 \pm 5.0	182.5 \pm 4.1	/	179.2 \pm 4.5

Data are mean \pm SD.

type sonicator at 220 W, 80% pulse mode, for 10 min. At the concentration of 2.5 mg/ml, TiO₂ nanoparticles agglomerated to a slightly larger size with larger standard deviation, while significant reduction of the secondary diameter of ZnO nanoparticles was found with comparison to the outcome of 0.5 mg/ml samples (Table 1).

Stability of suspension

Suspensions of TiO₂ and ZnO nanoparticles at concentration of 0.5 mg/ml were dispersed by a cup-type sonicator at 100 or 220 W, 80% pulse mode, for 10 min. The size distributions conducted soon after, and at 1, 3, and 7 days post-sonication are listed in Table 2. The secondary diameter of TiO₂ nanoparticle agglomerates increased by 4.7%, 7.8% and 9.2% when dispersed at 100 W, and by 1.5%, 5.9% and 4.5% at 220 W, respectively. As to ZnO nanoparticles, the secondary diameter increased by 1.9% and 3.4% (1 and 7 days post-sonication, respectively) at 100 W, and by 1.3% and 0.6% at 220 W.

Dispersion of MWCNTs

Dispersion of suspensions of MWCNTs at a concentration of 2.0 mg/ml was operated using the protocol: cup-type sonicator at 100 W, 80% pulse mode, for 10 min. The dispersion status was assessed using optical microscopy and TEM. Highly agglomerated masses of MWCNTs were dispersed into smaller size clusters after a single dispersion process (Fig. 8 (a) and (b)) and MWCNTs bundles were separated homogeneously by sonication for another 10 min (Fig. 8 (c)). Individual and bundled nanotubes were observed in samples sonicated twice in the TEM micrographs (Fig. 8 (d)).

Discussion

The present study used direct probe-type and indirect cup-type sonicator to prepare nanomaterials suspensions and subsequent size characterization was completed by DLS instrument and TEM. The effects of factors including

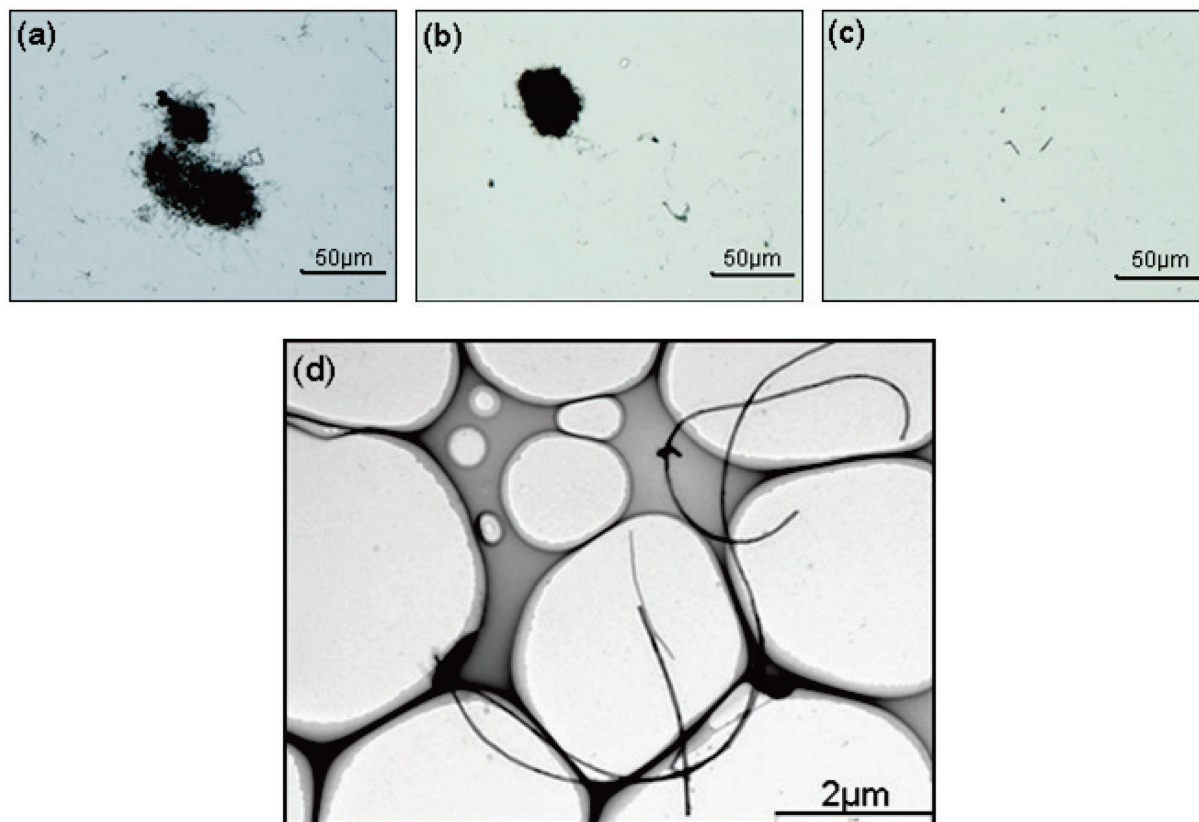


Fig. 8. Optical microscope micrographs of MWCNT suspensions at concentration of 2.0 mg/ml: (a) un-dispersed, (b) dispersed by a cup-type sonicator at 100 W, 80% pulse mode, for 10 min, and (c) for another 10 min; and (d) TEM micrograph of MWCNT sonicated twice.

particle concentration, dispersion time and output power of sonication on the dispersion status were investigated. Then a protocol was established and demonstrated to be suitable and reproducible for nanomaterials dispersion in terms of both size distribution and suspension stability.

Prior to the evaluation of dispersion condition, adjustment of appropriate particle concentration for DLS measurement was performed following the recommendations of the instrument instructions. According to the instructions, particle concentration is a factor for the accuracy of measurement, and sufficient opaqueness is suggested to accommodate the optical requirements of DLS. TiO₂ nanoparticles showed the smallest hydrodynamic diameter and deviation at the concentration of 25 μg/ml. At higher or lower concentrations than 25 μg/ml, variability of hydrodynamic diameter became greater, probably due to instable translational diffusion coefficient of Brownian motion resulting from changes in particle interaction. Although further study is needed to ensure whether the measured diameter was concentration dependent or not, the concentration of 25 μg/ml was optimal for size char-

acterization of TiO₂ nanoparticles with regard to the least deviation. By contrast, smaller peak 1 and especially lower PDI were observed in samples of higher concentration of ZnO nanoparticles. The higher PDI value derived from lower concentrations can be explained by the bimodal size distribution. Because of the similar refractive index between ZnO nanoparticles and DM, the light scattering intensity of DM turned out to be a certain proportion of the total recorded intensity and the quality of resulting DLS data was too poor to be interpreted correctly. In this situation, the light scattering intensity of nanoparticles could be enhanced by using elevated particle concentration, and good quality of DLS data was obtained at the concentration of 500 μg/ml in the present study. In case of size distribution with more than one peak, z-average, which is calculated from total detected intensity, is not suitable for description of particle size distribution. It is therefore advisable to use peak 1, the peak value of the principal peak of the intensity-weighted hydrodynamic diameter distribution, to compare the outcomes of DLS. It is worth noting that determination of proper concentration should

be conducted for each nanomaterial and the selected concentration should be reported.

Direct probe-type sonicator is usually recommended over indirect bath/cup-type sonicator based on the higher efficacy in energy delivery into the suspension, without energy loss generated from the process that ultrasonic waves pass through both the bath/cup liquid and the wall of the sample container, and thus is widely used in safety research on nanomaterials^{4, 10, 39, 40}). However, large variance is often encountered due to technical problems such as uncertainty in probe immersion position. Moreover, direct immersion of the probe into the suspension could introduce contamination of the sample at the same time. Although such contamination could be avoided, an unavoidable side effect of the probe-type is tip erosion, which was observed in our study. In addition, tip erosion also induces reduction of energy²¹), resulting in subsequent alteration of dispersion condition that is critical to data reproducibility. Furthermore, samples are usually left on the bench in uncovered containers. Thus, the evaporative loss of liquid content and deposition of dust should be taken into consideration as well.

On account of the aforementioned problems with probe-type sonicator, the cup-type sonicator was utilized for further analysis. Effective energy delivery was achieved by minimal interspace between the sample container and the internal layer of the cup, which contributed to significant minimization of energy loss. Simultaneously, due to the massive collapse of the bubbles and the high local energy generated, excessive heating cycles occur at the interface of the explosion. A rapid rise in liquid temperature is an inherent effect in both direct and indirect sonication²¹). In order to avoid overheating of the suspension along with consequent liquid evaporation or degradation of the medium components, a circulatory cooling system was used in this study. Smaller agglomerates and better monodispersion of TiO₂ nanoparticles was produced within shorter dispersion time by sonication at cooling water temperature of 5°C rather than -10°C. It is speculated that if the cooling water is set at an extremely low temperature, the cup-type sonicator may be frozen by the circulation, and this may induce inefficiency of sonication, resulting in subsequent poor dispersion of TiO₂ nanoparticle suspension. Moreover, effect of medium temperature on the particle interaction and size distribution needs to be studied further.

Besides the impact of temperature of cooling water, dispersion time and output power of sonicator play important roles in nanomaterials dispersion as well. Decrease in the

secondary dynamic diameters of TiO₂ and ZnO nanoparticles resulted from increased dispersion time or output power using probe-type or cup-type sonicator, respectively. This suggested that more delivered energy which was derived from increased dispersion time or output power of sonicator contributed to break the bonds within agglomerates and disrupt the formation of agglomeration. The asymptotic behavior of the size change with output power of sonicator observed in the present study is consistent with the findings of previous studies^{13, 41}). The secondary diameters ceased to change after a critical output power value, indicating that nanomaterials in suspensions cannot be dispersed to their primary sizes and that the presence of at least a minimal number of agglomerates should always be expected in safety research^{21, 38}).

In actual nanosafety research, samples with different concentrations of nanomaterials are required for dose-response experiments. Thus, we tested the effect of particle concentration on size distribution. TiO₂ and ZnO nanoparticles were sonicated at concentration of 0.5 or 2.5 mg/ml, and the size characterization was conducted. As a result, particle concentration at 0.5 or 2.5 mg/ml did not show an obvious effect on size distribution of TiO₂ nanoparticles, while reduction of the secondary diameter of ZnO nanoparticles was observed at higher concentration. In principle, higher particle concentration leads to increased particle collision frequency which can enhance particle breakage but also induce agglomerate formation at the same time. The discrepancy between TiO₂ and ZnO nanoparticles is due to the different physiochemical properties of each material, including different breakage behavior and/or surface interaction with components of the medium^{21, 22}). Such issues need to be investigated in future studies. The results highlight the demand to characterize the size distribution when dispersion of specific particles is operated at different concentrations. It is also important to report the dispersion concentration to allow comparisons between studies from different laboratories.

Stable dispersion status is usually desirable for studies spanning over days. Therefore, the stability of TiO₂ and ZnO nanoparticles suspension was assessed until the 7th days after sonication. Agglomerates of TiO₂ and ZnO nanoparticles increased slightly by only 10% and 5%, respectively, which was acceptable for safety evaluation of nanomaterials. Furthermore, alteration of output power from 100 to 220 W did not change the size distribution of TiO₂ and ZnO nanoparticles soon after sonication and both prevented the reagglomeration of nanoparticles for at least 7 d after dispersion. Since the sample was extremely

heated when sonicated for more than 10 min, dispersion time was limited to 10 min. Thus sonication can be operated with the maximum output power of 220 W for more energy delivery, but the results of stability demonstrated that desired degree of particle dispersion can be achieved with less output power of 100 W. In order to avoid overloading the sonicator and to minimize unwanted side effects²¹⁾, we established the best dispersion protocol as followed: cup-type sonicator, with output power of 100 W, 80% pulse mode, for 10 min.

The protocol was set up based on TiO₂ and ZnO nanoparticles and further application to dispersion of MW-CNTs was checked. Size characterization of nanotubes by DLS is not accurate²¹⁾, and thus optical microscopy and TEM were used for morphological observation. MWCNTs clusters were not able to be disrupted after one single sonication following this protocol. After cooling, another 10-min sonication was performed and MWCNTs were dispersed into smaller bundles consequently. As previously demonstrated in the section that described the effect of dispersion time, higher energy was delivered into the suspension by prolonged dispersion time to break the bonds within the agglomerates of nanoparticles, indicating that this procedure can also be applied to nanotubes. With regard to the side effect of temperature, the dispersion time should be extended by repeating the 10-min sonication rather than selecting continuous operation in the present cup-type sonicator protocol.

It is worth mentioning that this protocol is not for all dispersion systems for different nanomaterials, media, sonicators, and sample containers. We here outlined the procedure and key points for a dispersion optimization study that is essential to start nanotoxicological research. Application of this protocol to other dispersion systems is feasible by adjustment of dispersion time, output power of sonicator or particle concentration.

Conclusions

Our study described a practical protocol using an indirect cup-type sonicator to prepare nanomaterial suspensions specifically for *in vivo* pulmonary exposure studies. TiO₂ and ZnO nanoparticles, together with MWCNTs were well dispersed in a biocompatible medium and were stable for 7 days after sonication following this protocol. The size distribution results were influenced by particle concentration for both sonication and DLS measurement. Dispersion time and output power affected dispersion status with regard to the delivered energy. Additionally,

appropriate temperature of cooling system appeared to be critical to sufficient dispersion with the cup-type sonicator. The cup-type sonicator might be recommended as a useful alternative to conventional bath-type sonicator or probe-type sonicator based on its effective energy delivery and assurance of suspension purity.

Acknowledgement

The authors thank Mr. Satoshi Ogawa for assistance with electron microscopy. This work was supported in part by grants from the Japan Society for the Promotion of Science (NEXT Program #LS056) and JST Strategic Japanese-EU Cooperative Program "Study on managing the potential health and environmental risks of engineered nanomaterials".

Disclaimer

The findings and conclusions in this report are those of the authors and do not necessarily represent the views of the National Institute for Occupational Safety and Health.

References

- 1) European Commission. Commission recommendation of 18 October 2011 on the definition of nanomaterial. <http://ec.europa.eu/environment/chemicals/nanotech/index.htm#definition>. Accessed August 3, 2012.
- 2) Donaldson K, Stone V, Tran CL, Kreyling W, Borm PJA (2004) Nanotoxicology. *Occup Environ Med* **61**, 727–8.
- 3) Warheit DB, Hoke RA, Finlay C, Donner EM, Reed KL, Sayes CM (2007) Development of a base set of toxicity tests using ultrafine TiO₂ particles as a component of nanoparticle risk management. *Toxicol Lett* **171**, 99–110.
- 4) Sager TM, Castranova V (2009) Surface area of particle administered versus mass in determining the pulmonary toxicity of ultrafine and fine carbon black: comparison to ultrafine titanium dioxide. *Part Fibre Toxicol* **6**, 15.
- 5) Ema M, Kobayashi N, Naya M, Hanai S, Nakanishi J (2010) Reproductive and developmental toxicity studies of manufactured nanomaterials. *Reprod Toxicol* **30**, 343–52.
- 6) Nel A, Xia T, Madler L, Li N (2006) Toxic potential of materials at the nano level. *Science* **311**, 622–7.
- 7) Sager TM, Kommineni C, Castranova V (2008) Pulmonary response to intratracheal instillation of ultrafine versus fine titanium dioxide: role of particle surface area. *Part Fibre Toxicol* **5**, 17.
- 8) Sager TM, Porter DW, Robinson VA, Lindsley WG, Schwegler-Berry DE, Castranova V (2007) Improved method to disperse nanoparticles for *in vitro* and *in vivo* investigation of toxicity. *Nanotoxicology* **1**, 118–29.

- 9) Yamamoto S, Shwe TTW, Ahmed S, Kobayashi K, Fujimaki H (2006) Effect of ultrafine carbon black particles on lipoteichoic acid-induced early pulmonary inflammation in BALB/c mice. *Toxicol Appl Pharmacol* **213**, 256–66.
- 10) Shvedova AA, Kisin ER, Mercer R, Murray AR, Johnson JV, Potapovich AI, Tyurina YY, Gorelik O, Arepalli S, Schwegler-Berry O, Hubbs AF, Antonini J, Evans DE, Ku BK, Ramsey D, Maynard A, Kagan VE, Castranova V, Baron P (2005) Unusual inflammatory and fibrogenic pulmonary responses to single-walled carbon nanotubes in mice. *Am J Physiol Lung Cell Mol Physiol* **289**, L698–708.
- 11) Wick P, Manser P, Limbach LK, Dattlaff-Weglikowska U, Krumeich F, Roth S, Stark WJ, Bruinink A (2007) The degree and kind of agglomeration affect carbon nanotube cytotoxicity. *Toxicol Lett* **168**, 121–31.
- 12) Maynard AD, Kuempel ED (2005) Airborne nanostructured particles and occupational health. *J Nanopart Res* **7**, 587–614.
- 13) Bihari P, Vippola M, Schultes S, Praetner M, Khandoga AG, Reighel CA, Coester C, Tuomi T, Rehberg M, Krombach F (2008) Optimized dispersion of nanoparticles for biological *in vitro* and *in vivo* studies. *Part Fibre Toxicol* **5**, 14.
- 14) Oberdörster G, Oberdorster E, Oberdorster J (2005) Nanotoxicology: an emerging discipline evolving from studies of ultrafine particles. *Environ Health Perspect* **113**, 823–39.
- 15) Tsuji JS, Maynard AD, Howard PC, James JT, Lam CW, Warheit DB, Santamaria AB (2006) Research strategies for safety evaluation of nanomaterials part IV: risk assessment of nanoparticles. *Toxicol Sci* **89**, 42–50.
- 16) Li Z, Hulderman T, Salmen R, Chapman R, Leonard SS, Young SH, Shvedova A, Luster MI, Simeonova PP (2007) Cardiovascular effects of pulmonary exposure to single-wall carbon nanotubes. *Environ Health Perspect* **115**, 377–82.
- 17) Muller J, Delos M, Panin N, Rabolli V, Huaux F, Lison D (2009) Absence of carcinogenic response to multiwall carbon nanotubes in a 2-year bioassay in the peritoneal cavity of the rat. *Toxicol Sci* **110**, 442–8.
- 18) Liang GY, Pu YP, Yin LH, Liu R, Ye B, Su YY, Li YF (2009) Influence of different sizes of titanium dioxide nanoparticle on hepatic and renal function in rats with correlation to oxidative stress. *J Toxicol Environ Health* **72**, 740–5.
- 19) Li JG, Li WX, Xu JY, Cai XQ, Liu RL, Li YJ, Zhao QF, Li QN (2007) Comparative study of pathological lesions induced by multiwalled carbon nanotubes in lungs of mice by intratracheal instillation and inhalation. *Environ Toxicol* **22**, 415–21.
- 20) Kobayashi N, Naya M, Endoh S, Maru J, Yamamoto K, Nakanishi J (2009) Comparative pulmonary toxicity study of nano-TiO₂ particles of different sizes and agglomerations in rats: different short- and long-term post-instillation results. *Toxicology* **264**, 110–8.
- 21) Taurozzi JS, Hackley VA, Wiesner MR (2011) Ultrasonic dispersion of nanoparticles for environmental, health and safety assessment—issues and recommendations. *Nanotoxicology* **5**, 711–29.
- 22) Murdock RC, Braydich-Stolle L, Schrand AM, Schlager JJ, Hussain SM (2008) Characterization of nanomaterial dispersion in solution prior to *in vitro* exposure using dynamic light scattering technique. *Toxicol Sci* **101**, 239–53.
- 23) Schulze C, Kroll A, Lehr CM, Schafer UF, Becher K, Schneckeburger J, Isfort CS, Landsiedel R, Wohlleben W (2008) Not ready to use—overcoming pitfalls when dispersing nanoparticles in physiological media. *Nanotoxicology* **2**, 51–61.
- 24) Wang J, Chen C, Liu Y, Jiao F, Li W, Lao F, Li Y, Li B, Ge C, Zhou G, Gao Y, Zhao Y, Chai Z (2008) Potential neurological lesion after nasal instillation of TiO₂ nanoparticles in the anatase and rutile crystal phases. *Toxicol Lett* **183**, 72–80.
- 25) Kayat J, Gajbhiye V, Tekade RK, Jain NK (2011) Pulmonary toxicity of carbon nanotubes: a systematic report. *Nanomedicine* **7**, 40–9.
- 26) Pauluhn J (2010) Multi-walled carbon nanotubes: approach for derivation of occupational exposure limit. *Regul Toxicol Pharmacol* **57**, 78–89.
- 27) Tong H, McGee JK, Saxena RK, Kodavanti UP, Devlin RB, Gilmour MI (2009) Influence of acid functionalization on the cardiopulmonary toxicity of carbon nanotubes and carbon black particles in mice. *Toxicol Appl Pharmacol* **239**, 224–32.
- 28) Johnston HJ, Hutchison GR, Christensen FM, Peters S, Hankin S, Stone V (2009) Identification of the mechanisms that drive the toxicity of TiO₂ particulates: the contribution of physicochemical characteristics. *Part Fibre Toxicol* **6**, 33.
- 29) Cho WS, Duffin R, Poland CA, Howie SEM, MacNee W, Bradley M, Megson IL, Donaldson K (2010) Metal oxide nanoparticles induce unique inflammatory footprints in the lung: important implications for nanoparticle testing. *Environ Health Perspect* **118**, 1699–706.
- 30) Holsapple MP, Farland WH, Landry TD, Monteiro-Riviere NA, Carter JM, Walker NJ, Thomas KV (2005) Research strategies for safety evaluation of nanomaterials, part II: toxicological and safety evaluation of nanomaterials, current challenges and data needs. *Toxicol Sci* **88**, 12–7.
- 31) Krug HF, Wick P (2011) Nanotoxicology: an interdisciplinary challenge. *Angew Chem Int Ed* **50**, 1269–78.
- 32) Driscoll KE, Costa DL, Hatch G, Henderson R, Oberdorster G, Salem H, Schlesinger RB (2000) Intratracheal instillation as exposure technique for the evaluation of respiratory track toxicity: uses and limitations. *Toxicol Sci* **55**, 24–35.
- 33) Osier M, Baggs RB, Oberdorster G (1997) Intratracheal instillation versus intratracheal inhalation: influence of cytokines on inflammatory response. *Environ Health*

- Perspect **105**, 1265–71.
- 34) Wallenborn JG, McGee JK, Schladweiler MC, Ledbetter AD, Kodavanti UP (2007) Systemic translocation of particulate matter-associated metals following a single intratracheal instillation in rats. *Toxicol Sci* **98**, 231–9.
- 35) Shinohara N, Nakazato T, Tamura M, Endoh S, Fukui H, Morimoto Y, Myojo T, Shimada M, Yamamoto K, Tao H, Yoshida Y, Nakanishi J (2010) Clearance kinetics of fullerene C₆₀ nanoparticles from rat lungs after intratracheal C₆₀ instillation an inhalation C₆₀ exposure. *Toxicol Sci* **118**, 564–73.
- 36) Warheit DB, Webb TR, Reed KL, Frerichs S, Sayes CM (2007) Pulmonary toxicity study in rats with three forms of ultrafine-TiO₂ particles: differential responses related to surface properties. *Toxicology* **230**, 90–104.
- 37) Rehn B, Seiler F, Rehn S, Bruch J, Maire M (2003) Investigations on the inflammatory and genotoxic lung effects of two types of titanium dioxide: untreated and surface treated. *Toxicol Appl Pharmacol* **189**, 84–95.
- 38) Porter D, Sriram K, Wolfarth M, Jefferson A, Schwegler-Berry D, Andrew M, Castranova V (2008) A biocompatible medium for nanoparticle dispersion. *Nanotoxicology* **2**, 144–54.
- 39) Hussain S, Thomassen LC, Ferecatu I, Borot MC, Andreau K, Martens JA, Fleury J, Baeza-Squiban A, Marono F, Boland S (2010) Carbon black and titanium dioxide nanoparticles elicit distinct apoptotic pathways in bronchial epithelial cells. *Part Fibre Toxicol* **7**, 10.
- 40) Lu S, Duffin R, Poland C, Daly P, Murphy F, Drost E, MacNee W, Stone V, Donaldson K (2009) Efficacy of simple short-term *in vitro* assays for predicting the potential of metal oxide nanoparticles to cause pulmonary inflammation. *Environ Health Perspect* **117**, 241–47.
- 41) Hielsher Y (2005) Ultrasonic production of nano-size dispersions and emulsions. *Dans European Nano Systems Workshop – ENS 2005*.